Atomistic simulation of plasticity in silicon nanowires

F. Cleri, T. Ishida, D. Collard, H. Fujita

Atomistic simulation of plasticity in silicon nanowires

Cite as: Appl. Phys. Lett. **97**, 153106 (2010); https://doi.org/10.1063/1.3501987
Submitted: 23 August 2010 • Accepted: 24 September 2010 • Published Online: 12 October 2010

Fabrizio Cleri, Tadashi Ishida, Dominique Collard, et al.

Atomistic simulation of plasticity in silicon nanowires

Fabrizio Cleri,[1,a)] Tadashi Ishida,[2] Dominique Collard,[2,3] and Hiroyuki Fujita[2]
[1]*Institut d'Electronique, Microelectronique et Nanotechnologie, CNRS, UMR 8520, Université de Lille I, F-59652 Villeneuve d'Ascq, France*
[2]*Institute of Industrial Science, University of Tokyo, Tokyo 153-8505, Japan*
[3]*Laboratory for Integrated Micro-Mechatronics Systems, CNRS-IIS (UMI 2820), University of Tokyo, Tokyo 153-8505, Japan*

(Received 23 August 2010; accepted 24 September 2010; published online 12 October 2010)

We study the tensile deformation of polycrystalline Si nanowires by means of molecular dynamics simulations. The initial microstructure is composed by a network of nanocrystals glued together by a thin layer of amorphous material. Atomistic simulations could clearly identify liquidlike flow in the constrained amorphous Si as the responsible for the observed elongation. After this first stage of nearly constant-stress flow, a necking instability sets in, eventually leading to fracture, at the point when the nanowire diameter becomes comparable to the size of the nanocrystals. © *2010 American Institute of Physics*. [doi:10.1063/1.3501987]

The possibility of a plastic response of silicon to mechanical stresses, and its brittle-to-ductile transition with temperature, have been the subject of intense research over the past twenty years,[1,2] due to the enormous technological relevance of this material. Plasticity in Si at temperatures below ~900 K is usually ruled out because of the high energy of the Peierls barrier to dislocation mobility.[3,4] However, despite such a common understanding, dislocation activity in Si has been reported during indentation experiments at room temperature in single crystals with a nanometer-scale geometry.[5] Moreover, large plastic deformation in excess of 100% was observed in single crystal Si nanowires under tensile loading,[6] and attributed to dislocation-initiated amorphization. Notably, a frequent observation in such nanoscale experiments[4–6] is the presence of an amorphous interlayer percolating within the Si nanocrystalline structure. Similarly, a network of nanocrystals embedded in an amorphous intergranular phase were found after severe mechanical deformation of polycrystalline Si.[7]

Such findings open the question of whether the mechanical behavior of nanostructured Si can be peculiar with respect to that of the bulk (both single- and polycrystalline) material. Previous theoretical studies[8] suggested that the large-scale elongation observed in a idealized model of nanocrystalline Si should be associated with the liquidlike flow of the amorphous interlayer. In this letter, we establish a strong support for such an indication, on the basis of the results of molecular dynamics (MD) simulations of tensile deformation of a realistic, finite-size Si nanowire, constructed as an assembly of nanocrystals embedded in a thin amorphous layer. The evolution of the crystalline and amorphous phases, and of the thin layer representing the interface, is the main factor driving the mechanical response. The results show a two stage stress-strain curve, whose first branch arises from the shear flow of the amorphous Si, with only a minor elastic contribution from the nanocrystals, and a second branch corresponding to strain hardening and necking of the weakest (amorphous) region, once the cross section of the finite-size nanowire has become comparable to the average grain size.

We performed MD simulations with the well known Stillinger–Weber interatomic potential for silicon.[9] A nanocrystalline structure with eight randomly oriented crystals of average radius $R_C = 1.8$ nm was prepared by following the same procedure already established for our previous nanocrystal MD simulations.[10] Subsequently, a fat cylinder including 60 960 Si atoms, with diameter and length $2R_0 = L_0 = 10.9$ nm, was cut from this structure. Constant-traction border conditions[11] were applied along the cylinder axis, to represent continuity with bulk Si while the lateral surface was free.

Increasing values of uniaxial strain were applied in steps of $\varepsilon = 10^{-3}$ at the temperature of $T = 300$ K. Although extremely time consuming, such simulations produce an average strain rate of about $\dot{\varepsilon} = 10^{7}$ s^{-1}, obviously much faster than in real experiments. Therefore, strain relaxation at constant stress was enhanced by periodically performing annealing cycles of 0.1 ns at $T \sim 900$ K, at about every 5% strain steps. Figure 1 shows a sequence of snapshots from three successive stages of such a computational deformation experiment. It is worth noting that our realistic nanocrystalline system could be representative of various experimental situations, e.g., a portion of a longer nanowire.[6]

Under such conditions, the simulated nanowire first underwent plastic yielding, around 13% strain, and then contin-

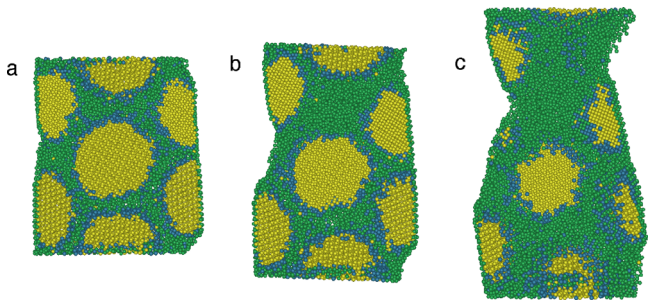

FIG. 1. (Color online) Snapshots of a central slice of the nanowire at (a) 15%, (b) 35%, and (c) 60% elongation, respectively. In the color version, yellow spheres indicate atoms in the crystalline grains; blue spheres atoms in the "defect accumulation layer;" and green atoms the constrained-amorphous phase. Colors are assigned according to the excess energy per atom, ΔU (in eV/atom), with respect to the energy of unstrained bulk Si: yellow, $\Delta U < 0.05$; blue, $0.05 < \Delta U < 0.15$; and green, $\Delta U > 0.15$.

a)Author to whom correspondence should be addressed. Electronic mail: fabrizio.cleri@univ-lille1.fr.

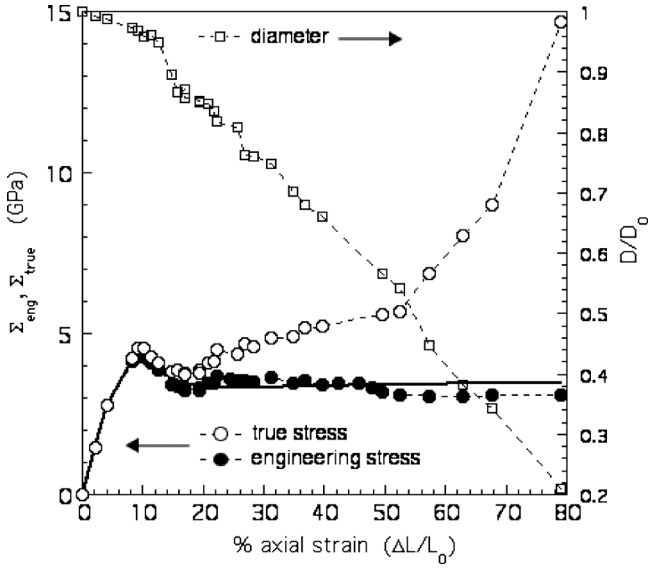

FIG. 2. Stress-strain data for a uniaxial tensile MD simulation of the nanostructured Si nanowire at $T=300$ K, with the Stillinger–Weber potential. Circles=engineering stress (black) and true stress (open, both on left-ordinate axis); squares (right-ordinate axis)=nanowire diameter. Dashed lines are a guide to the eye. The full curve represents the fit from Eq. (1) in the text.

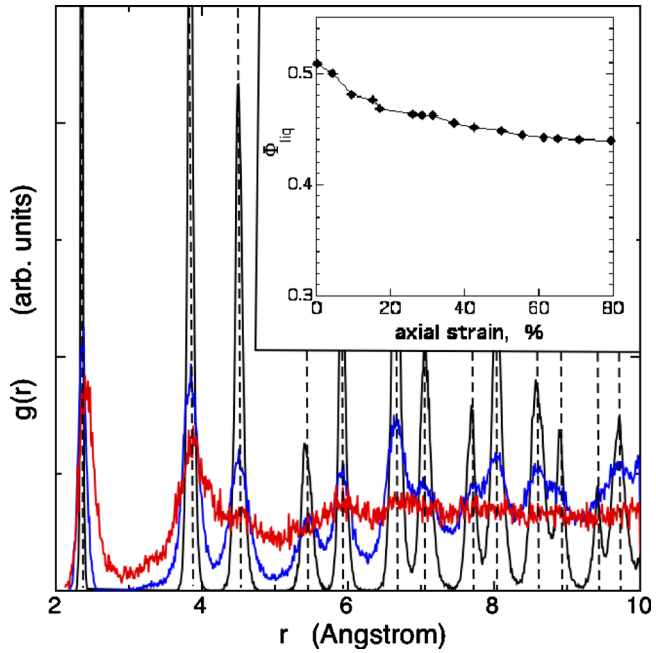

FIG. 3. (Color online) Pair-distribution function $g(r)$ from the MD simulations, for the crystalline phase (black), amorphous phase (red), and defect-accumulation layer (blue), at 35% tensile deformation and $T=300$ K. Vertical dashed lines represent the crystalline peaks at $T=0$ and zero strain. Inset: evolution of the liquidlike mass fraction Φ_{liq} with respect to the total mass of the amorphous phase, with increasing uniaxial strain.

ued the elongation at nearly constant stress up to ~55% strain. Direct observation of the atomic configurations around this point shows that a necking instability in the amorphous region sets in. After this point, the true stress (i.e., stress divided by the actual cross section) quickly rises, corresponding to the rapid reduction in the neck diameter, up to a final fracture strain of >80%, when the nanowire breaks by ductile tearing. A typical stress-strain curve from such a numerical experiment is shown in Fig. 2. Notably, the finite size of the system in the transverse direction is a crucial element to observe this behavior.

After the brief linear-elastic phase, our nanowire follows a quasistatic creeplike response up to a strain of about 60%. This behavior is similar to what described in MD simulations of bulk nanocrystalline Si under strain.[8] In this stage, our nanocrystalline structure clearly shows three distinct, evolving regions as follows: a crystalline region (C, corresponding to the interior of each nanocrystal); a "constrained" amorphous region (A, the percolating network among different nanocrystals); and a defect-accumulation layer (D, a thin shell surrounding each nanocrystal). The three regions can be clearly distinguished according to various signatures, e.g., the pair-distribution function, $g(r)$ (Fig. 3), energy-density, or bond-angle distributions.

The intergranular material (A) takes up most of the flow deformation in this stage. At the same time, the C regions merely adjust to the surrounding flow while losing some material by amorphizing along the boundaries. During the deformation, the energy stored does not involve a significant elastic deformation of the nanocrystals. In fact, none of the neighbor peaks in the $g(r)$ distribution of Fig. 3 change in the C regions by more than 1%, even upon straining the system by as much as 40%–60%, upon comparison with the $g(r)$ at zero strain, only a minor broadening of the peaks is noticeable. Looking at the energy distributions, we see that most of the input energy goes into the A region, plus some fraction into the D-layer. Notably, the latter is still very nearly crystalline, however, the peaks are much broadened. Inside the A region the energy is converted into shearlike flow, with local rearrangement of the atoms but the short range structure remaining that of the plain amorphous Si [see again the $g(r)$]. The energy in the D-layer is used to increase the number of defects, and to partly transform into the A phase. During transformation in the D-layer, the fraction of A is slowly increased while the average grain size slowly decreases. These observations are also confirmed by following the repartition of the elastic energy among the three phases, which closely follows the time evolution of the concentration fractions of A-, C-, and D-regions. The above results should be qualitatively reproducible also by other Si interatomic potentials, since at the low temperatures explored most existing potentials are known to give equivalent descriptions of the various phases.

The final part of the true stress-strain curve rises abruptly, with a "hardening" effect up to the final fracture. The critical diameter at which necking sets in indicates that the size of the amorphous region in the nanowire, somewhere along the nanowire length, has become comparable to the average size of the nanocrystals. At such critical diameter, the nanowire contains regions in which the nanocrystals are separated only by amorphous material. Stress can be concentrated in such nonconstrained, fully amorphous region, where necking can be initiated. Now, the bulklike amorphous material (differently from the constrained amorphous interlayer) can be shear-strained up to fracture, like a single-phase material. Atoms in the A phase were characterized all along the strain path by means of the two parameters μ and σ introduced in Ref. 12, and "solidlike" and "liquidlike" fractions could thereof be obtained. The inset of Fig. 3 shows the evolution upon increasing strain of the liquidlike mass fraction Φ_{liq}. The microscopic origin of the observed strain hard-

ening could be traced back to the sizeable decrease in the denser, liquidlike component, since the latter was already indicated[12] as the main carrier of plasticity in amorphous Si. It is worth noting that our two-phase, finite-size nanowire can never be considered to be at steady state, hence the decrease in Φ_{liq} even below the "asymptotic" value, $\Phi_0=0.46$, obtained for an infinite bulk amorphous Si.[12]

The existence of a thermodynamically stable disordered structure ("constrained amorphous") of the grain boundaries in nanocrystalline materials and notably in Si, was revived some time ago.[13,14] More recent simulations contend that, at $T=0$ K, the grain-boundary structures must be ordered, and may turn into a somewhat disordered state, however distinct from the amorphous state, at higher temperatures.[15] In the present case, the reason for the amorphouslike disordering can be found in the highly random orientations, and in the very small size, of the grains. Both factors enhance the interfacial excess energy, also helping a possible kinetic trapping of the interfacial amorphous phase. Polycrystalline Si severely deformed by ball milling[7] clearly exhibits a two-phase structure, with nanocrystals of ~ 8 nm size embedded in 15 vol % of amorphous Si. Under similar conditions, steady-state creep was observed in computer simulations of pure Si.[8,16] As noted before, the distinction between *constrained* and *free* amorphous material is crucial to our description of mechanical properties of the nanostructure.

The stress-strain data from the MD simulation can be fitted by a spring-and-dashpot two-phase curve (full line in Fig. 3), describing the stress distribution among the A- and C-region as follows (the contribution of the D layer being negligible):

$$\sigma(\varepsilon) = \sigma_C(\varepsilon)\exp(-u\varepsilon^2) + \sigma_A(\varepsilon)[1-\exp(-u\varepsilon^2)], \qquad (1)$$

with $\sigma_C(\varepsilon)=\varepsilon Y/(1+\nu)$ and $\sigma_A(\varepsilon)=k\varepsilon^{1+\alpha}$. The best-fit values of the parameters are $u=130$, $k=3.5$, and $\alpha=-0.96$, with u measuring the relative weight of the two components and k giving the asymptotic stress value. Stress in crystalline Si follows a standard linear-elastic deformation law, however with effective Young's modulus $Y=95$ GPa and Poisson's ratio $\upsilon=0.25$, to account for the fraction of noncrystalline material present; while at larger strains, and before necking, the constrained amorphous Si dominates with its weak (the stress exponent α being close to zero) creeplike stress dependence.

In summary, our deformation model lends substantial support to the indication that large-scale elongation in Si nanocrystalline structures is to be associated with the liquidlike flow of the amorphous interlayer, constrained within the elastically deforming nanocrystals. While it is likely that dislocations may participate in the early stages of plastic deformation,[6] the widespread presence of a constrained-amorphous second phase, percolating within the nanocrystalline Si structure, appears to be the crucial element to understand plasticity in nanocrystalline silicon. Experimental demonstrations of large-strain plasticity in Si would represent a major technological breakthrough, allowing the molding of Si nanostructures into complex shapes, for a large number of applications.

[1] P. B. Hirsch and S. G. Roberts, Philos. Mag. A **64**, 55 (1991).
[2] C. Scandian, H. Azzouzi, N. Maloufi, G. Michot, and A. George, Phys. Status Solidi C **171**, 67 (1999).
[3] H. Alexander and P. Haasen, Solid State Phys. **22**, 27 (1969).
[4] S. G. Roberts and P. B. Hirsch, Philos. Mag. **86**, 4099 (2006).
[5] A. M. Minor, E. T. Lilleodden, M. Jin, E. A. Stach, D. Chrzan, and J. W. Morris, Philos. Mag. **85**, 323 (2005).
[6] X. Han, K. Zheng, Y. Zhang, X. Zhang, Z. Zhang, and Z. L. Wang, Adv. Mater. (Weinheim, Ger.) **19**, 2112 (2007).
[7] T. D. Shen, C. C. Koch, T. Y. Tsui, and G. M. Pharr, J. Mater. Res. **10**, 2892 (1995).
[8] M. J. Demkowicz, A. S. Argon, D. Farkas, and M. Frary, Philos. Mag. **87**, 4253 (2007).
[9] F. H. Stillinger and S. K. Weber, Phys. Rev. B **19**, 2112 (1984).
[10] S. R. Phillpot, P. Keblinski, F. Cleri, and D. Wolf, Interface Sci. **7**, 15 (1999).
[11] F. Cleri, Phys. Rev. B **65**, 014107 (2001).
[12] M. J. Demkowicz and A. S. Argon, Phys. Rev. Lett. **93**, 025505 (2004).
[13] D. Wolf, in *Handbook of Materials Modeling*, edited by S. Yip (Kluwer, Dordrecht, 2005), Vol. 1, Chap. 6.13.
[14] P. Keblinski, S. R. Phillpot, D. Wolf, and H. Gleiter, Phys. Lett. A **226**, 205 (1997).
[15] S. von Alfthan, K. Kaski, and A. Sutton, Phys. Rev. B **76**, 245317 (2007).
[16] V. Yamakov, D. Wolf, M. Salazar, S. R. Phillpot, and H. Gleiter, Acta Mater. **50**, 61 (2002).